IEEE Access
Multidisciplinary | Rapid Review | Open Access Journal

Received December 15, 2020, accepted December 27, 2020, date of publication January 18, 2021, date of current version January 28, 2021.

Digital Object Identifier 10.1109/ACCESS.2021.3051411

High Impedance Single-Phase Faults Diagnosis in Transmission Lines via Deep Reinforcement Learning of Transfer Functions

HAMID TEIMOURZADEH[1], (Student Member, IEEE), ARASH MORADZADEH[1], (Student Member, IEEE), MARYAM SHOARAN[1], BEHNAM MOHAMMADI-IVATLOO[1], (Senior Member, IEEE), AND REZA RAZZAGHI[2], (Member, IEEE)

[1]Faculty of Electrical and Computer Engineering, University of Tabriz, Tabriz 5166616471, Iran
[2]Department of Electrical and Computer Systems Engineering, Monash University, Melbourne, VIC 3800, Australia

Corresponding author: Behnam Mohammadi-Ivatloo (mohammadi@ieee.org)

ABSTRACT Accurate and fast fault detection in transmission lines is of high importance to maintain the reliability of power systems. Most of the existing methods suffer from false detection of high-impedance faults. In this paper, the transfer function (TF) method is introduced to evaluate the effect of impedance and location of faults by analyzing the voltage and current signals in the frequency domain. Interpretation of the results of the TF method is considered as a weakness of this method. In order to alleviate this problem, a convolutional neural network (CNN) and the hybrid model of deep reinforcement learning (DRL) are utilized to identify and locate single-phase to ground short circuit faults in transmission lines. Single-phase to ground short circuit faults with various fault impedances are applied on an IEEE standard transmission line system. Then, the TF traces are calculated and are collected as input datasets for the proposed models. The fault location results for each network are evaluated via various statistical performance metrics such as correlation coefficient (R), mean squared error (MSE), and root mean squared error (RMSE). The R-value of the CNN and DRL models in fault identification is presented as 96.12% and 98.04%, respectively. Finally, in the early detection of single-phase to ground short circuit fault location (high impedance), the results revealed the efficiency of the DRL model with R=96.61% compared to CNN with R=95.21%.

INDEX TERMS Transmission line faults, single-phase to ground short circuit, transfer function, deep reinforcement learning, convolutional neural network.

I. INTRODUCTION

Transmission lines are crucial components in power systems. With recent innovations, conventional electric power systems have been evolving into intelligent power systems, consist of advanced monitoring and control tools [1]. Transmission lines are always prone to faults due to various reasons, including lightning or falling objects. Whenever a fault occurs, the nominal values of voltage and current deviates in the power system, which causes equipment damage and power outages [2]. Reliable, efficient algorithms capable of providing an accurate analysis of the type and location of faults in transmission lines are necessary for the implementation of power transmission protection systems [3].

The associate editor coordinating the review of this manuscript and approving it for publication was Fanbiao Li.

Within the context of power system protection, detection of high impedance faults is recognized to be extremely challenging [4]. This is due to the fact that these faults do not significantly affect the voltage and current characteristics. Indeed, the effect of these faults might be seen as an additional load [5]. Nonetheless, the detection of these faults is of high importance as they could cause serious safety risks and could adversely affect the quality of power supply. There are practically two types of high impedance faults that can be considered: (i) a broken live conductor directly touching the ground, (ii) a close connection to earth like sweeping the earth through trees or damaged insulation. As power systems are becoming more complicated and with more stringent power quality constraints, detection of high impedance faults has become a major concern for utilities [6]. On the other hand, the involvement of uncertainties in fault information

has caused some problems in the operation of fault diagnosis methods [7], [8]. These uncertainties are mainly classified into three categories: 1) different faults cases exhibit a complex set of features and diverse behaviors, challenging the implementation of protection schemes based on a single fault feature [9], [10]; 2) the instability of the operating conditions can cause problems for protection schemes adjusted with a pre-defined setting value [11]; 3) due to high fault impedance, the currents produced by the faults are not usually sufficient to be detected by common protection devices [12], [13]. In traditional protection systems, the protection relay trips the system once the operating parameter deviates from a preset threshold. However, the settings of traditional protection relays are computed offline and are not configurable during operation. This adjustment method is unable to adjust to different types of faults, meaning that the relay settings are required to adapt to the new system conditions online. The common protection schemes with a fixed setting strategy have shown to be unreliable for protection of power systems [14]. In fact, fixed relay settings can seriously hinder the development of power system protection technology.

The single phase-to-ground fault is the most common fault type in power systems, most of which are accompanied by a fault impedance at the point of failure [15]. High fault impedance values can result in the failure or mal-operation of the power system protection devices, which in turn results in jeopardizing the power system's reliable operation [16]. Studies on improving the safety of power protection systems against fault impedance are classified into three categories. 1) improving the protection performance against fault impedance through adaptive adjustment of setting value [17]. For example, in [11], the operating threshold is automatically adjusted based on the fault impedance and according to the compensated voltage variation. In [18], the authors proposed a scheme to prevent failures in line protection performance in response to the dominant conditions of the system. 2) compensating the fault impedance such that the measured impedance can more accurately reflect the fault location [19]. For example, to enhance the performance against the fault impedance, in [20] the authors proposed a fault line impedance consideration process. The fault line impedance, additional impedance, and contained impedance are shifted together in the multiple levels until the additional impedance matches with the actual way of the true axis. The fault distance and fault line impedance are calculated following the regular connection between the shifted fault line impedance and the shifted calculated impedance in the multiple levels. Another type of impedance compensation has been done in [21], in which the authors first tried to perform improved ground-type impedance relay by compensating spread capacitive currents then the description of internal high-resistance faults is done while ensuring reliability under external faults. In [22], the impact of fault impedance on the performance of distance relays protecting radial distribution feeders has been studied. In [23], the fault impedance was calculated based on the active power at the relay point. The measured excess impedance was then compensated such that the fault location could be more accurately located by the measured impedance. Based on the fact that the sequence current phase measured at the relay point is almost equal to that at the point of failure, the authors in [24] expressed the measured impedance by decomposing it into two components, namely resistance and a reactance term. Moreover, by combining both terms, the fault impedance is eliminated, and the real fault impedance is calculated. 3) identification of internal and external faults based on the characteristics of the fault impedance. For example, in [25], the criterion for protection against a high-resistance single line-to-ground fault on the transmission lines is based on the differential active power principle which can accurately identify a high-resistance single line-to-ground fault. The authors in [26] propose an intelligent method for fault localization based on the information provided by PMUs. The fault segment is first discovered by analyzing the waveforms of the zero-sequence current on both sides of the fault. A stack auto-encoder (SAE) is then formed to implement an end-to-end strategy to determine the fault point through voltage and current phasors.

Nowadays, data mining and artificial intelligence (AI) play a significant role in modern power systems. Data mining techniques such as artificial neural networks (ANNs), machine learning, deep learning, and fuzzy logic are widely employed for operational tools such as monitoring, management, and fault identification. The AI systems are widely known for their high ability to identify the type and location of faults in power systems.

In [27], the authors used a quality-aware fine-grained categorization model called Fast R-convolutional neural network (CNN) that is suitable for category tips learning. This paper aims to identify the most distinguished image spots for classification of faults.

In [28], for managing the relationship among electrical signals at one side and fault data on transmission lines, authors suggest the purpose of independent neural networks. This technique allows an automated adjustment of the neural models qualified for fault classification, location, and detection. The hidden Markov model (HMM) algorithm is used in [29] for fault classification in power transmission lines. The basis of this method is the direct analysis of electrical signals in the form of multivariate time series. In [30], applications of recurrent neural network (RNN), long short-term memory (LSTM), and support vector machine (SVM) are utilized for data-based line trip fault prediction in power systems. The first one mainly responsible for obtaining the transient characteristics of multi-sourced data and the other one is considered for classification to acquire the ultimate prediction outcomes.

The authors of [31] proposed an anti-heat dynamic assessment approach based on the LSTM technique. In this study, the cluster features of the power-angle path of a generator are received as the input after the fault is eliminated, and the modified LSTM is then employed to learn the nonlinear

relationships between input properties and transient stability. At the same time, the time sliding windows and the anti-heat mechanism are utilized to develop a real-time orderly prediction framework capable of effectively using the time series data of PMUs.

One of the major drawbacks in most of the above-mentioned methods is that the diagnosis operation is not performed accurately and the proposed solutions have an error due to the high-dimension of monitored data. To solve this problem, in [32], [33], solutions based on dimension reduction and data processing are presented.

In this paper, single-phase short circuit faults detection, and exact location are identified in two scenarios. The first scenario calculates the transfer function (TF) of each fault to identify the presence of the fault in the system by comparing the calculated TFs. In the second scenario, in order to identify the exact location of single-phase short-circuit faults in transmission lines, the deep reinforcement learning (DRL) method is proposed as one of the hybrid applications of deep learning and reinforcement learning. In addition to its high ability to extract data properties, the proposed method also improves the idea of hybrid models. To the best of the authors' knowledge, this method has not been used to recognize patterns in TFs of single-phase short circuit faults and diagnose the exact location of transmission line faults. The calculation of the TFs clearly shows all the effects of the faults on the voltage and current signals in a frequency domain. The proposed hybrid model of DRL, by recognizing the patterns and extracting the features in the TFs, it will be able to identify the exact location of the single-phase short-circuit fault in a transmission line.

The rest of this paper is organized as follows. The second section describes the TF method. In Section III, the proposed methodologies are introduced. Section IV describes the system under study. In Section V, the results of the assessment and identifying the fault location are presented in two scenarios. Finally, Section VI concludes the paper.

II. TRANSFER FUNCTION METHOD

The transfer function (TF) method is a comparative test to diagnose defects, especially in transient states. So far, this method has been widely used in power industry, e.g., [34]–[38], including detection of mechanical defects in power transformer windings [34], [39], diagnostic operations in electrical machines [36], and detection of distribution network damages [37], [38], [40]. Since this method examines the changes in a system in the frequency domain, in most literature, this method has been introduced as a frequency response analysis. A comparison of the healthy and damaged states transfer functions of the system is the basis of this method in identifying defects.

In this paper, the TFs related to the system are calculated as following [37]:

$$TF = \left| \frac{FFT(V_t)}{FFT(I_t)} \right| \tag{1}$$

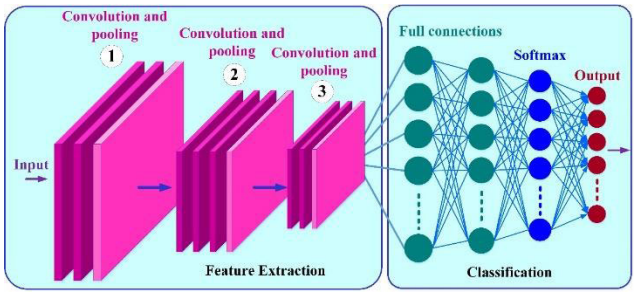

FIGURE 1. Principle structure of CNN.

where $FFT(V_t)$ and $FFT(I_t)$ are the voltage and current of the system, both in the frequency domain using fast Fourier transfer (FFT). The voltage and current signals are extracted in the EMTP software. Then, Fourier Transform of voltage and current signals are calculated.

The TF method can display the slightest effects of the faults, even for very high-impedance faults on the TF trace. Despite all the advantages of this method, the interpretation of the TF traces is challenging and requires experienced specialists. Hence, in this paper, a convolutional neural network (CNN) and the hybrid method of DRL are suggested for interpreting the TF traces and extracting the features of them. The proposed hybrid approach will be able to accurately categorize and localize the single-phase to ground faults via extracting the features of its TFs.

III. METHODOLOGIES

In this section, we first describe the CNN. Then, the DRL is presented.

A. CONVOLOTIONAL NEURAL NETWORK (CNN)

CNN is one of the powerful deep learning architectures, which is mainly used as a tool for feature extraction, pattern recognition, classification problems, and image processing. CNN inherently extracts features or patterns based on the convolution operator. For extracting features, it benefits from ideas such as local connections, shared weight, integration and multi-layered structure [41], [42]. As shown in Fig. 1, convolutional layers, pooling layers, and fully-connected layers are form the CNN structure. Each layer plays a unique role in this structure until the feature extraction operation is performed in the best possible way [43].

Each convolution layer, in its own structure, includes filters that identify the features in the input data. Convolution operation occurs by passing inputs from each filter. Each filter can introduce several features [44]. Basic CNN uses conventional activation functions such as the sigmoid activation function, in which case it needs to calculate an exponent. In dealing with high nonlinear data, this issue will have problems such as increased training and evaluation times.

To prevent this problem, CNN uses a nonlinear activation function $f(x) = max(0, x)$ called Rectified Linear Unit (ReLU) in each convolution layer. The convolutional layer

utilizes a ReLU that is defined in the following [42], [45]:

$$x_j^l = f\left(\sum_{i\in M_j} x_i^{l-1} * k_{ij}^l + b_j^l\right) \tag{2}$$

where x_j^l shows the product of the j-th filter in l-th convolutional layer; f is a nonlinear activation function, operator $*$ shows convolution, k_{ij}^l denotes the convolutional kernel of the l-th layers between the i-th input and the j-th output feature maps, and b_j^l defines the bias.

After performing the convolution stage in CNN, another important stage is pooling. A pooling operation is a form of sub-sampling of the convolution layer with a summary statistic. Average pooling and Max pooling are two types of pooling operations. The average pooling takes the average value of the extracted features and transfers it to the next convolution layer, so most commonly utilized in CNN is max-pooling. Max Pooling issues the maximum values for each sub-region outputs by dividing the input data into a set of non-overlapping rectangles. The pooling layer has effective advantages for CNN, such as reducing the free variables for reaching the dimensionality reduction and ensure the invariance to shift and distortion. The pooling layer is formulated as the following form [42], [45]:

$$x_j^l = f\left(\beta_j^l pooling\left(x_j^{l-1}\right) + b_j^l\right) \tag{3}$$

where operator $pooling()$ demonstrates the pooling stage and β is the pooling kernel.

Convolutional and max-pooling layers are known as the center of the CNN. After extracting the features of the input data via several end-to-end convolutional and pooling operations, the upper-layers are consisting of fully-connected layers same as a multilayer perceptron (MLP) neural network in order to calculate the weight and scores of the inputs or extracted features [41], [45]. Finally, the classification of the features is done using a Softmax function after fully-connected layers in the last part of the CNN structure as follows [41]:

$$O_j = \begin{bmatrix} P(y=1)|x;\theta \\ P(y=2)|x;\theta \\ \cdots \\ P(y=c)|x;\theta \end{bmatrix} = \frac{1}{\sum_{j=1}^{c}\exp(\theta^j x)} \begin{bmatrix} \exp(\theta^1 x) \\ \exp(\theta^2 x) \\ \cdots \\ \exp(\theta^c x) \end{bmatrix} \tag{4}$$

where $\theta^j x$ denotes the factors of the classification layer and c represent the number of classes.

B. DEEP REINFORCEMENT LEARNING (DRL)

RL is an important application of machine learning. The task of RL can usually be described as a Markov decision process (MDP). As shown in Fig. 2, RL has four important components such as agent, environment, action (At), and reward (Rt). Gaining ideal experience through the interaction between the environment and the agent can be described as the main idea of RL [46], [47].

RL operates based on the sustainable environment knowledge with a feedback loop for quality and appropriate decisions. It should be noted that RL is a well-known learning

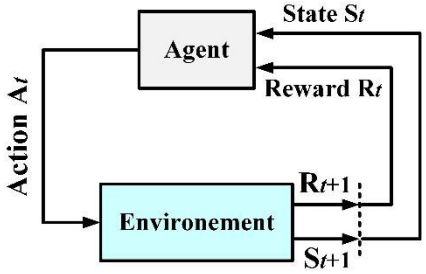

FIGURE 2. Reinforcement layer structure.

algorithm based on the agent so that the agent behaves by performing work and achieving results in the environment. Trial-and-error search and delayed reward are two main features of RL [47]. Trial-and-error search indicates the occurrence of a trade-off between exploration and exploitation. Preferably, the agent wants to use the effective actions taken in the past to generate the reward, however, the agent must discover better new actions that may have a higher reward in the future. By trying different actions, the agent should gradually support those who receive the most rewards [48], [49]. Recently, solving RL problems has been improved by adding multilayer neural networks to their structure, which is known as DRL. The powerful ability of the deep neural network in pattern recognition, feature extraction, image processing has increased the efficiency of RL. Deep Q-networks (DQNs) are one of the powerful DLRs algorithms proposed in 2013. High accuracy, stability and high speed of the training process are the most important advantages of this model [50], [51]. Identifying and correctly diagnosing samples in the training data is the principal idea of the classification agent. The classification agent with accurate and high-precision diagnoses includes positive rewards. Therefore, it will be able to achieve its goal by maximizing the cumulative rewards at [52]:

$$g_t = \sum_{k=0}^{\infty} \gamma^k r_{t+k} \tag{5}$$

where, γ is the discount factor to balance the immediate and future reward, r_t is the reward at time t and shows the feedback from the environment.

Through it, the success or failure of the agent's actions can be measured. In DQN, a function called the Q function is as follows, which calculates the quality of a mode-action combination [52].

$$Q^{\pi}(s,a) = E_{\pi}\left[g_t \,|s_t = s, a_t = a\right] \tag{6}$$

where s demonstrates the current state and a represents the action. During the DQN training process, in order to reflect the result of the agent-environment interaction in the action value function (AVF) (s,a), an update of the action value of the function is performed by collecting the experience data set by the agent. Using the following Bellman equation, a duplicate update process is formed from the AVF [51].

$$Q_{t+1}(s,a) = max_{a'} E\left[r + \gamma max_{a'} Q_t\left(s', a'\right)\middle| s, a\right] \tag{7}$$

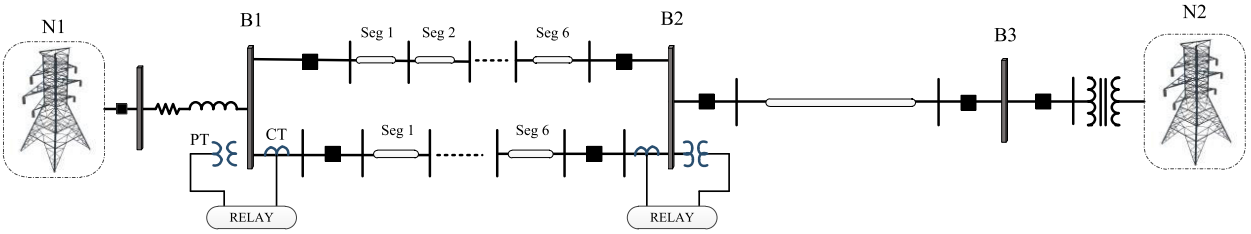

FIGURE 3. The schematic representation of the network model.

where s' is the next time-step of s and a' depicts the action accomplished by the agent at the next time-step.

In DQN, designating an action is perform with the optimal AVF $Q^*(s, a)$ as the following equation that determines the optimal action.

$$Q^*(s,a) = max_\pi E\left[r_t + \gamma r_{t+1} + \gamma^2 r_{t+2} + \ldots \mid s_t = s, a_t = a, \pi\right] \quad (8)$$

where π as a classification policy is a function that receives a sample and returns probabilities of all labels.

Q functions cannot be solved in high-dimensional continuous mode space. It is essential to present a deep Q-learning algorithm that fits the Q function with a deep neural network to solve this problem. The AVF (s, a) can be approximated as $(s, a; \theta)$ by using a CNN with the parameter θ. So, using the loss function $L(\theta)$, the action value network can be iteratively updated [52], [53].

$$L(\theta) = \sum_{(s,a,r,s')\epsilon B} (y - Q(s,a;\theta))^2 \quad (9)$$

where y shows the predicted target of the Q function and it is defined as [52]:

$$y = r + (1-b)\gamma \sum_{a'} Q(s', a'; \theta_t) \quad (10)$$

where $b = 1$ if terminal=True; otherwise $b = 0$, and θ_t represent a parameter for the target action value of the separate deep neural network. The derivative of the loss function $(L(\theta))$ according to θ is as [52]:

$$\frac{\nabla L(\theta)}{\nabla(\theta)} = -2 \sum_{(s,a,r,s')\epsilon B} (y - Q(s,a;\theta)) \frac{\nabla Q(s,a;\theta)}{\nabla Q} \quad (11)$$

Optimal Q* function is now achieved by minimizing the loss function. Then greedy policy gets the maximum cumulative reward under the optimal Q* function. Finally, the optimal classification policy $\pi*$ is achieved [52], [53].

IV. CASE STUDIES

To evaluate the performance of the proposed method, the power system shown in Fig. 3 is considered. The model consists of two networks represented by N1 and N2. As demonstrated in Fig. 3, there are two 230kV transmission lines. The first one, which connects B1 to B2 is a double-circuit line and the second one is a single-circuit line between B2 and B3. Each transmission line distance is 45 miles,

TABLE 1. Tower configuration for 230kV double-circuit line.

Conductor	HSR(ft)	Height at Tower (ft)	Height at mid spam(ft)
1	0.0	100.0	73.0
2	0.0	83.5	56.5
3	0.0	67.0	40.0
4	29.0	67.0	40.0
5	29.0	83.5	56.5
6	29.0	100.0	73.0

TABLE 2. Tower configuration for 230kV single-circuit line.

Conductor	HSR(ft)	Height at Tower (ft)	Height at mid spam(ft)
1	0.0	100.0	73.0
2	0.0	83.5	56.5
3	0.0	67.0	40.0

and both of the lines are divided into six parts. Constant and lumped parameter line models are utilized in modeling of double and single-circuit lines, respectively. Table 1 and 2 represents the parameters of tower configuration for 230kV double-circuit line and the tower configuration for 230kV single-circuit line, respectively.

More details on the network information are accessible at [54]. The system is simulated in ATP/EMTP environment.

V. SIMULATION RESULTS

In this study, single-phase to ground faults are investigated in various segments of a transmission line by applying the faults with different impedances. To apply the fault, the transmission line is divided into six equal parts, each segment (seg) containing 16.66% of the line. In each seg of this line, single-phase to ground fault are created in each phase with the fault impedance of 1, 50, 100, 500, 1000, 3000, and 5000 Ohms.

Then, the voltage and current signals for each faulty state are measured and recorded. The stochastic nonlinear current caused by arcing and nonlinear characteristics of high impedance faults have different effects on transient and steady-state responses of the power system. Thus, these effects are used as a criterion for the fault detection. Hence, appropriate models of fault impedance need to be considered that are able to represent nonlinearity, asymmetry, and the

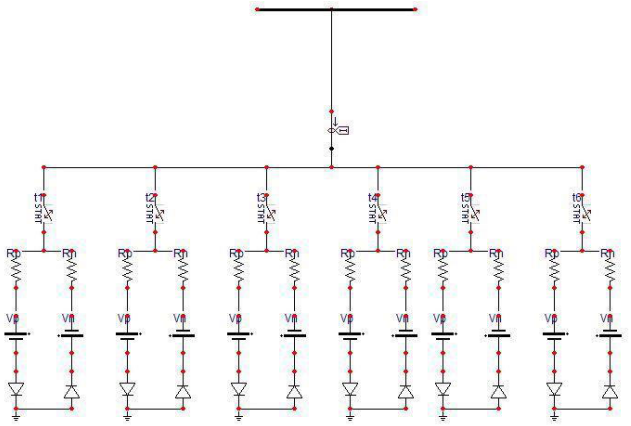

FIGURE 4. High impdance fault model based on a number of Emanuel arc model.

TABLE 3. Arcs Parameters of HIF.

parameter	T(on\off)	R_p	R_n	V_p	V_n
Arc 1	0.06	1500	1505	9000	10000
Arc 2	0.08	9000	9600	8000	9000
Arc 3	0.12	6500	7000	11000	11050
Arc 4	0.14	5800	6500	12000	12500
Arc 5	0.1	10000	11100	2000	2050
Arc 6	0.16	5300	6200	11000	11500

low frequency of high impedance fault currents. In this paper, an Emanuel arc model [55] has been used. In Fig. 4, the EMTP-based simulation model for a high impedance fault is presented. All parameters for 6 arcs are shown in Table 3. Fig. 5 shows the line segments and faults in each seg of the transmission line. After applying various faults, their identification and location are performed in two different steps using the TF method and deep learning applications. Each of the steps is introduced in the following.

A. STEP 1: IDENTIFYING SINGLE-PHASE TO GROUND SHORT CIRCUIT FAULT VIA THE TF METHOD

In this step, the TF method is used to identify and analyze existing faults. To this end, the equation (1) is utilized to calculate the TF related to the intact and damaged states to illustrate the effects of the fault on the voltage and current signals on the TF traces. Note that the sampling frequency in all steps based on the Nyquist - Shannon Theorem is equal to 28 kHz. Fig. 6 shows the TF related to the intact state of the studied system. Fig. 7 illustrates the TF traces for single-phase to ground short-circuit faults with 1-Ohm resistance in all segments of the transmission line. The TFs related to single-phase to ground short circuit faults are presented in the second seg of the transmission line with the all types of mentioned fault impedances in Fig. 8.

Figs. 7 and 8 show the effect of the location and impedance of the fault on the TF traces, respectively. Comparing the TFs and observing the variations in their amplitude and frequency ranges indicates that there is a fault in the system. According to Fig. 8, it can be observed that with increasing the impedance of fault, changes in the TFs tend to be similar to the intact state TF, making it difficult to detect high impedance faults. Identifying faults in early stages (high impedance faults) can ensure system stability and prevent serious damages to transmission lines and other equipment. Achieving this goal and locating and accurately identifying high-impedance faults requires a precise and robust method for interpreting the TF traces. In this paper, the interpretation of TF traces and the achievement of this important diagnosis method is made using deep learning applications called CNN and DRL in step 2.

B. STEP 2: LOCALIZATION AND CATEGORIZATION OF SINGLE PHASE TO GROUND SHORT CIRCUIT FAULTS BY DEEP LEARNING APPLICATIONS

In this step, deep learning applications are used to interpret the TF traces. Interpreting the TFs and extracting their features will ensure accurate classification and localization of faults. For this purpose and based on the idea of hybrid models, the hybrid method of DRL is presented in this paper. In addition, the CNN method is applied to the same data to compare the results of both methods. Fig. 9 shows the flowchart of the proposed method for diagnosis transmission line faults. Using learning methods in the first step requires a dataset. TF traces are collected and utilized as a data matrix.

Transmission lines are divided into 6 segments, and in each phase of each segment, single-phase to ground short-circuit faults is tested with 7 different impedance values. Thus, the data matrix consists of 253 traces (126 faulty traces related to internal faults, 126 faulty traces corresponding to external faults, and one trace related to intact state). For internal faults, the location of each fault is considered as the target number (regardless of the severity of the fault) and is assigned a zero target number for the trace of intact state. For external faults related to segs 1 to 6 of the test system, the numbers of 7 to 12 are considered as target, respectively. In the network training and test stages, each *seg* of the transmission line is defined as a class. Zero number class is also assigned to the TF of the intact state. After designing the networks and determining the dataset as the input of each network, 70% of the data is determined for training and the rest for the test. In the meantime, the selection of training and test data is made randomly by the network itself. Each of the designed networks is trained with relevant data and uses test data to validate the training. After training and testing, the performance and results for each network are evaluated via statistical performance metrics. In this paper, correlation coefficient (R), mean absolute error (MAE), and root mean squared error (RMSE) are used to evaluate the performance of each network. How to calculate each of these metrics is as

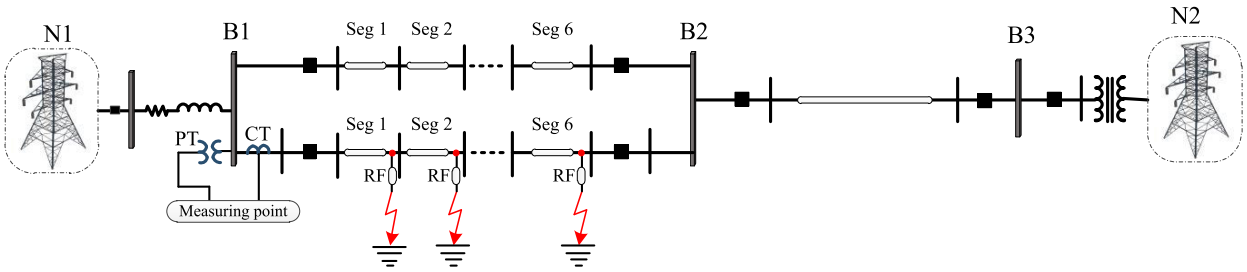

FIGURE 5. Implementation of single-phase to ground short circuit faults the on transmission line.

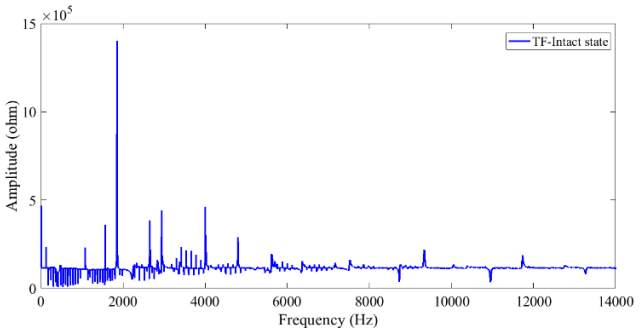

FIGURE 6. TF associated with the intact state of the transmission line.

follows [56], [57]:

$$R = \frac{\sum_{i=1}^{N}\left(X_i - \bar{X}\right)\left(Y_i - \bar{Y}\right)}{\sqrt{\sum_{i=1}^{N}\left(X_i - \bar{X}\right)^2 \sum_{i=1}^{N}\left(Y_i - \bar{Y}\right)^2}} \quad (12)$$

$$MSE = \frac{1}{N}\sum_{i=1}^{N}(X_i - Y_i)^2 \quad (13)$$

$$RMSE = \sqrt{\frac{1}{N}\sum_{i=1}^{N}(X_i - Y_i)^2} \quad (14)$$

where X_i, $\bar{X}$, Y_i, and $\bar{Y}$ illustrate the real value, average of real values, predicted value, and average of predicts values, respectively. Figs. 10 and 11 show the results of identifying and categorizing single-phase to ground faults by the DRL model for training and test data, respectively.

The results presented in Fig. 10 show the network training with a high correlation coefficient (R=9851). When the network is trained with high accuracy, it means that it has been able to extract outstanding features of the data and know their patterns well. It is also observed that the designed network is able to distinguish data related to external faults from the internal single-phase to ground short circuit faults related to the same segment. The results provided for network testing are also acceptable, and the test phase and location detection of single-phase to ground short circuit faults for test data have been performed with a high correlation coefficient ($R = 0.9804$). Fig. 12 shows the MSE and RMSE errors for the testing stage of the DRL network. It should be noted that the error values of MSE and RMSE for the training stage of the DRL were zero. The training and test steps

TABLE 4. Comparison of training and test results provided by CNN and DRL.

	Train			Test		
Method	R	MSE	RSME	R	MSE	RSME
CNN	0.9799	0.5148	0.7174	0.9638	0.7805	0.8834
DRL	0.9851	0.4257	0.6524	0.9804	0.7058	0.8401

for identifying and classifying single-phase to ground short circuit faults were performed by CNN, and the results of R, MSE, and RMSE of the CNN are presented in Table 4. This table also compares the results of both the CNN and DRL methods in diagnosing single-phase to ground short circuit faults.

The results presented in Table 5 show the accuracy and efficiency of the proposed methods for detecting and locating single-phase to ground short circuit faults in the transmission line. It can be seen that the proposed hybrid method of DRL has been able to pass the training and testing stages more accurately than the CNN method and provide better results.

One of the important parameters of short circuit faults is the fault inception angle (FIA) (ranging from 0 to 90 degrees). In this paper, in order to evaluate the performance of the proposed method against the FIA, single phase to ground short circuit faults with the inception angles of 30, 60, and 90 degress are also tested in each seg of the test system. The TFs associated with each fault are calculated and used as the test data for trained networks. Figs. 13, 14, and 15 show the detection results for faults with the inception angles of 30, 60, and 90, respectively.

It is observed that the proposed method is able to distinguish faults with different inception angles. The networks were trained with the zero inception angle faults and are able to detect faults with the inception angles of 30, 60, and 90 with the R values of 0.9760, 0.9680, and 0.9600, respectively.

Fault detection during power swing can be very challenging. In order to assess the performance of the proposed method against the power swing, faults with the power swing are generated in the test system and their TFs are calculated and selected as test data for trained networks. Fig. 16 shows the detection results for the power swing faults.

The results presented in Fig. 16 show the accurate performance of the proposed method in identifying single-phase to

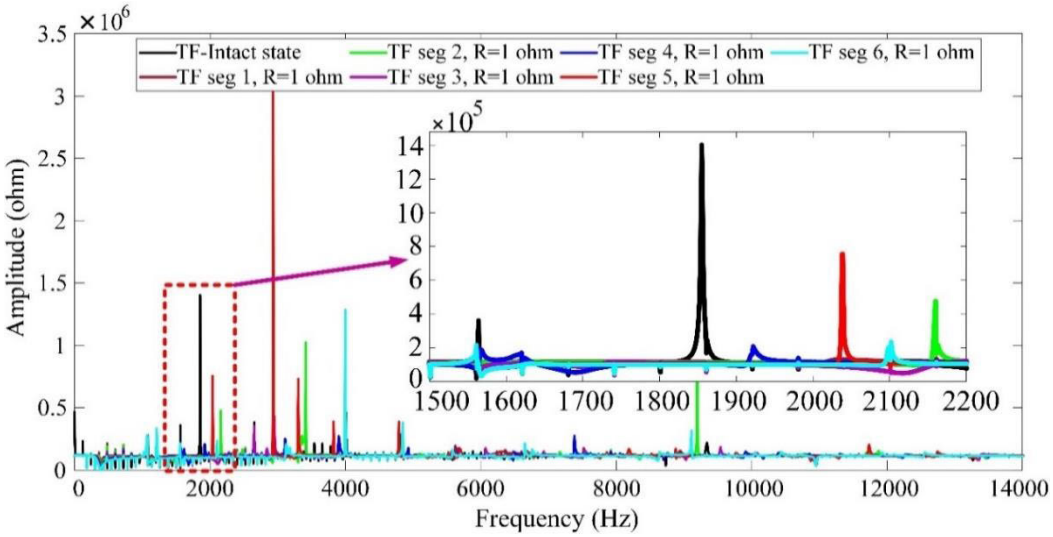

FIGURE 7. TFs related to low-impedance single-phase to ground short circuits in all segments of transmission lines.

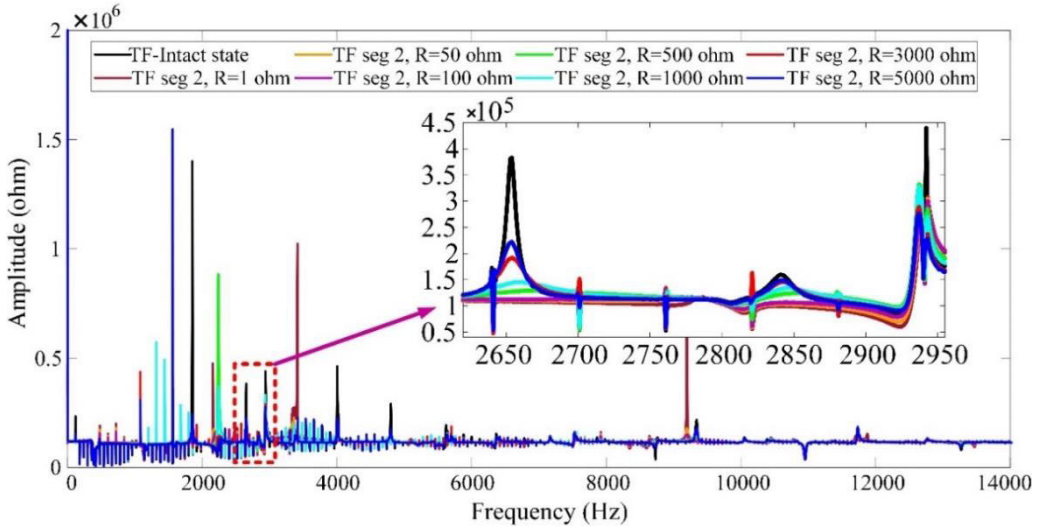

FIGURE 8. Changes in TFs due to various short circuit resistances in segment 2 of transmission lines.

ground short circuit faults in the presence of power swing in the test system. It is observed that the trained network is able to provide R value of 0.9680 in this prediction.

The nature of the power system and its topology can change by altering the short circuit levels at both ends power systems. However, the protection system must be able to operate accurately despite changes in the short-circuit fault level. In order to assess the performance of the proposed method, single phase to ground short circuit faults are applied in each seg of the test system under two conditions, (i) equal sources and (ii) stronger remote source. The TFs related to the tested faults in each condition were considered as test dataset for the trained network. Figs. 17 and 18 show the fault detection results under two mentioned conditions, respectively.

The results presented in Figs. 17 and 18 show that the proposed method has a satisfactory performance against the change in the nature of the power system and its topology due to changes in the short circuit level. The proposed method was able to detect system faults in terms of equal resources with the R values of 0.9840 and in conditions of stronger remote source with the R values of 0.9520.

It should be noted that due to the fact that the detection and identification of single-phase to ground short circuit faults in the early stages (high impedance) is very valuable and is one of the goals of this paper. High impedance faults are identified in the following of this section. To do this, in each seg of this line, single-phase to ground short circuit fault were tested in each phase with impedance values of 300, 7000, and 9000 Ohms. Then, the voltage and current signals for each

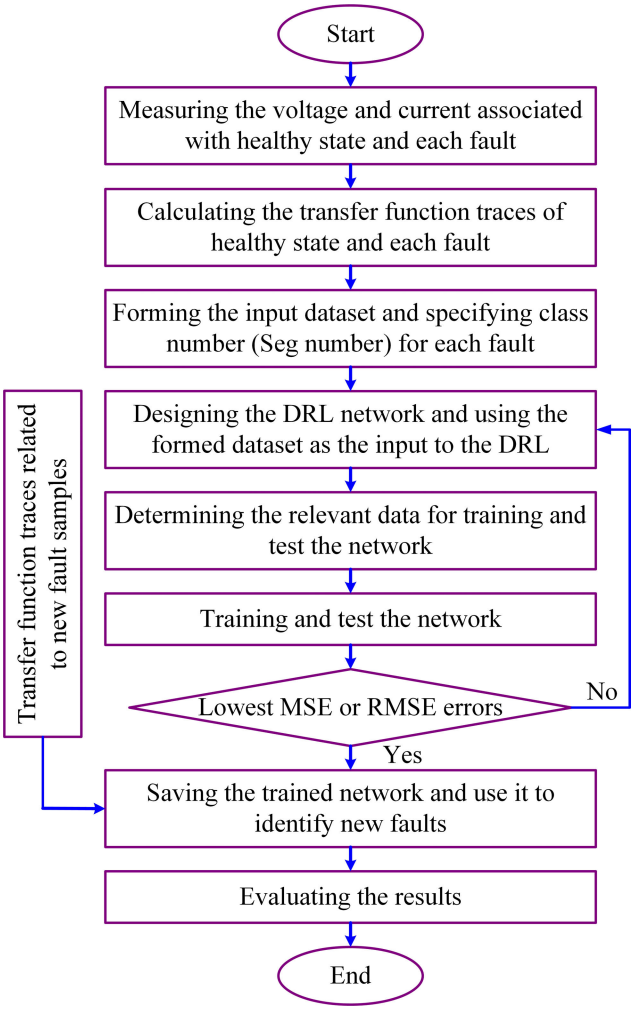

FIGURE 9. Flowchart of the proposed fault diagnosis technique.

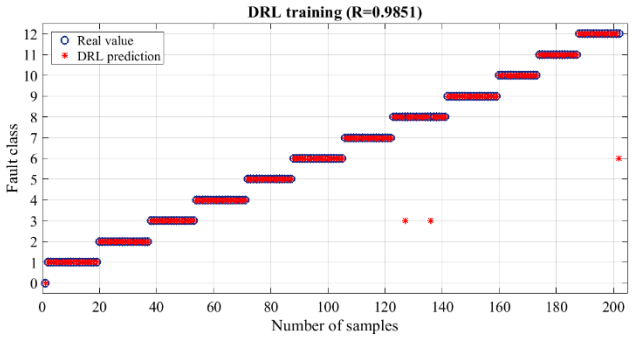

FIGURE 10. Identification and classification of faults by DRL in the training stage.

fault were recorded. The TF related to each of these faults were calculated and used as input for each of the trained networks. Tables 5 and 6 show the results of identifying and locating new and unknown faults by CNN and DRL, respectively.

In fault detection operations in power systems, one of the most important issues is the detection time. The use of deep learning and machine learning applications in fault detection

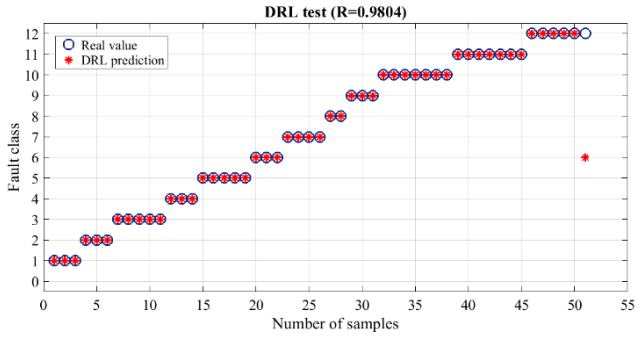

FIGURE 11. Identification and classification of faults by DRL in the testing stage.

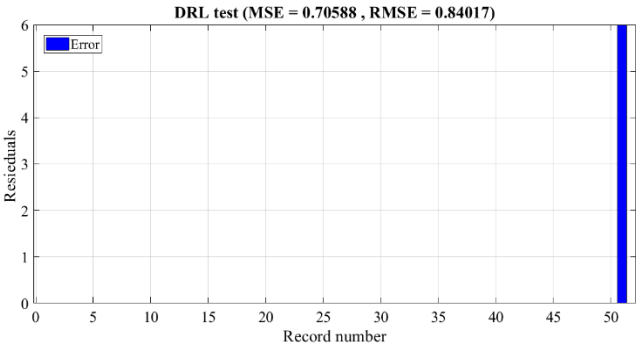

FIGURE 12. MSE and RMSE errors for the testing stage of DRL.

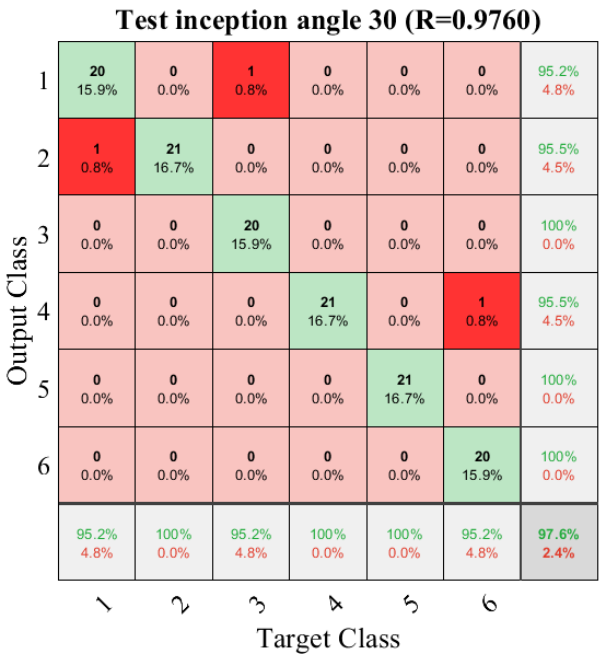

FIGURE 13. Detection of single phase to ground short circuit faults by considering the phase angle 30.

operations, in addition to reducing computational complexity, has also significantly reduced fault detection time compared to other conventional and traditional methods. In these methods, due to the difference in the performance of the training

TABLE 5. Diagnosis and locating new single-phase to ground short circuit faults (high impedance) via CNN.

Real value	Impedance	CNN prediction	Real value	Impedance	CNN prediction	Real value	Impedance	CNN prediction
	R=300 Ω	1		R=300 Ω	2		R=300 Ω	3
1-a-g	R=7000 Ω	1	2-a-g	R=7000 Ω	2	3-a-g	R=7000 Ω	3
	R=9000 Ω	0		R=9000 Ω	0		R=9000 Ω	2
	R=300 Ω	1		R=300 Ω	2		R=300 Ω	3
1-b-g	R=7000 Ω	1	2-b-g	R=7000 Ω	2	3-b-g	R=7000 Ω	3
	R=9000 Ω	2		R=9000 Ω	2		R=9000 Ω	2
	R=300 Ω	1		R=300 Ω	2		R=300 Ω	3
1-c-g	R=7000 Ω	1	2-c-g	R=7000 Ω	2	3-c-g	R=7000 Ω	3
	R=9000 Ω	1		R=9000 Ω	3		R=9000 Ω	3
	R=300 Ω	4		R=300 Ω	5		R=300 Ω	6
4-a-g	R=7000 Ω	4	5-a-g	R=7000 Ω	5	6-a-g	R=7000 Ω	6
	R=9000 Ω	5		R=9000 Ω	4		R=9000 Ω	6
	R=300 Ω	4		R=300 Ω	5		R=300 Ω	6
4-b-g	R=7000 Ω	4	5-b-g	R=7000 Ω	5	6-b-g	R=7000 Ω	6
	R=9000 Ω	3		R=9000 Ω	5		R=9000 Ω	6
	R=300 Ω	4		R=300 Ω	5		R=300 Ω	6
4-c-g	R=7000 Ω	4	5-c-g	R=7000 Ω	5	6-c-g	R=7000 Ω	6
	R=9000 Ω	4		R=9000 Ω	6		R=9000 Ω	4

TABLE 6. Diagnosis and locating new single-phase to ground short circuit faults (high impedance) via DRL.

Real value	Impedance	DRL prediction	Real value	Impedance	DRL prediction	Real value	Impedance	DRL prediction
	R=300 Ω	1		R=300 Ω	2		R=300 Ω	3
1-a-g	R=7000 Ω	1	2-a-g	R=7000 Ω	2	3-a-g	R=7000 Ω	3
	R=9000 Ω	1		R=9000 Ω	0		R=9000 Ω	3
	R=300 Ω	1		R=300 Ω	2		R=300 Ω	3
1-b-g	R=7000 Ω	1	2-b-g	R=7000 Ω	2	3-b-g	R=7000 Ω	3
	R=9000 Ω	1		R=9000 Ω	2		R=9000 Ω	4
	R=300 Ω	1		R=300 Ω	2		R=300 Ω	3
1-c-g	R=7000 Ω	1	2-c-g	R=7000 Ω	2	3-c-g	R=7000 Ω	3
	R=9000 Ω	0		R=9000 Ω	3		R=9000 Ω	3
	R=300 Ω	4		R=300 Ω	5		R=300 Ω	6
4-a-g	R=7000 Ω	4	5-a-g	R=7000 Ω	5	6-a-g	R=7000 Ω	6
	R=9000 Ω	2		R=9000 Ω	5		R=9000 Ω	6
	R=300 Ω	4		R=300 Ω	5		R=300 Ω	6
4-b-g	R=7000 Ω	4	5-b-g	R=7000 Ω	5	6-b-g	R=7000 Ω	6
	R=9000 Ω	4		R=9000 Ω	5		R=9000 Ω	6
	R=300 Ω	4		R=300 Ω	5		R=300 Ω	6
4-c-g	R=7000 Ω	4	5-c-g	R=7000 Ω	5	6-c-g	R=7000 Ω	6
	R=9000 Ω	4		R=9000 Ω	6		R=9000 Ω	6

and test stages, the operating time of each is also different. In this paper, the training time for the CNN and DRL is 62.41s and 37.86s, respectively. The test stage or single phase to ground short circuit detection are performed by each of the CNN and DRL networks in 0.9s and 0.5s, respectively. It should be noted that this time is related to identifying the total fault samples of each dataset at each stage. Each of the CNN and DRL techniques detects each fault sample in 0.014 s and 0.009 s, respectively. The calculations performed and the time obtained for fault detection are performed in a ASUS system with the CPU of Intel Core i7-3630QM, 2.4GHz, and the fault detection time can be various in the use of other systems.

After testing each of the trained and saved networks using new and high-impedance faults, Table 7 shows the results of this step for both CNN and DRL by R, MSE, and RMSE metrics. Also, this table provides a comparative approach to results of single-phase to ground short circuit fault detection

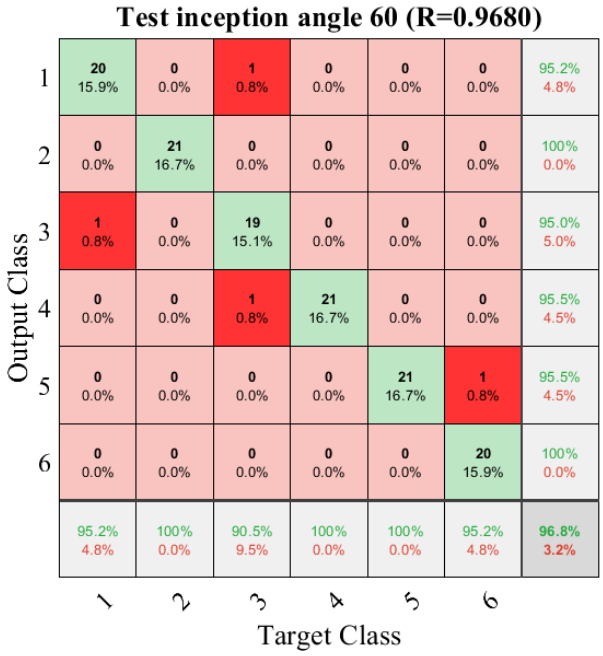

FIGURE 14. Detection of single phase to ground short circuit faults by considering the phase angle 60.

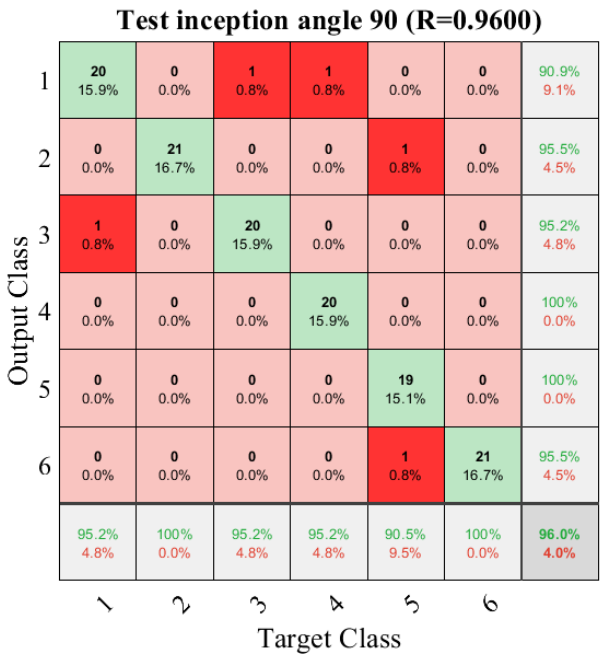

FIGURE 15. Detection of single phase to ground short circuit faults by considering the phase angle 90.

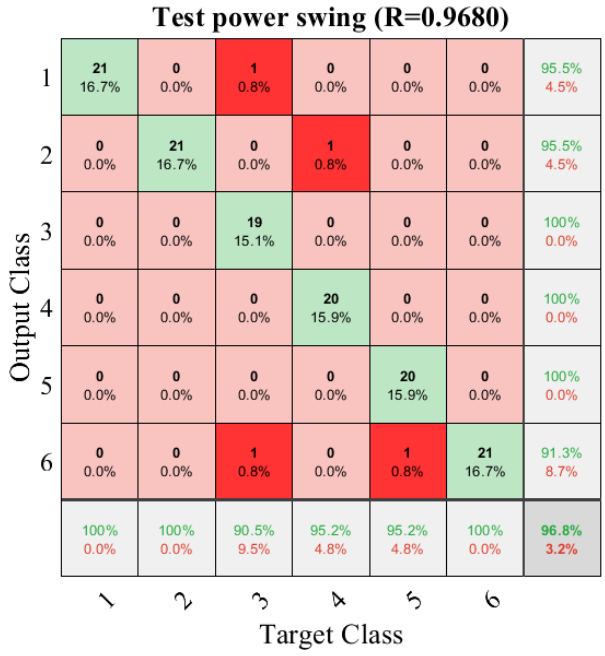

FIGURE 16. Detection of single phase to ground short circuit faults by considering the power swing.

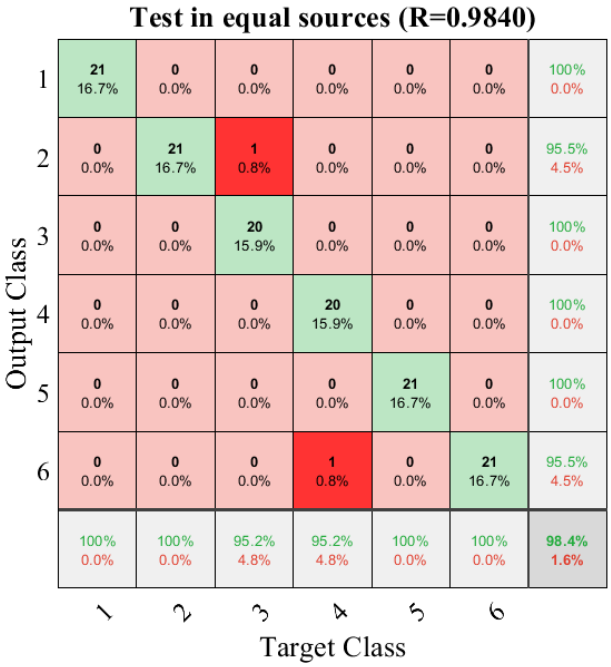

FIGURE 17. Detection of single phase to ground short circuit faults by considering sources in equal conditions.

in transmission line for the methods used in this paper and other solutions presented in other studies.

Based on the results presented in Table 7, it can be seen that the trained networks were, in most cases, able to detect and locate high impedance faults. Comparing the results of the proposed methods, it was observed that the CNN method with 95.21% accuracy and DRL method with 96.61% accuracy were able to locate new and unknown faults. At this stage, the results confirmed the superiority and efficiency of the proposed hybrid model of DRL in detecting the single-phase to ground short circuit faults. Interpretation of TF traces using learning methods can be the best step in locating transmission line faults and be important in improving condition monitoring issues of the power system. Finally, it should be noted that the suggested methods in this paper are also applicable for real-world data.

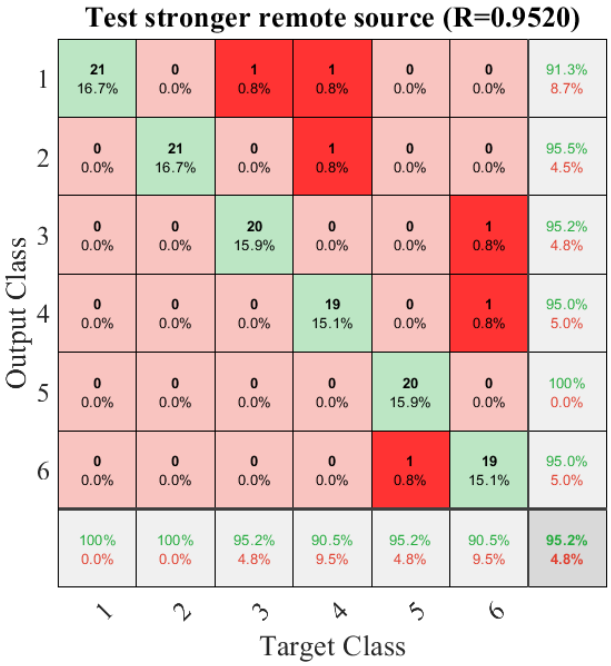

FIGURE 18. Detection of single phase to ground short circuit faults by considering remote source in stronger state.

TABLE 7. Comparison of the results of different methods in detecting the single-phase to ground short circuit fault in the transmission line.

	High impedance fault			Low impedance fault		
Method	**R**	**MSE**	**RSME**	**R**	**MSE**	**RSME**
CNN	0.9521	0.2963	0.5443	0.9638	0.7805	0.8834
DRL	0.9661	0.2222	0.4713	0.9804	0.7058	0.8401
HMM [29]	-	-	-	0.9000	-	-
SVM+LSTM [30]	-	-	-	0.9770	-	-
Fast R-CNN [27]	0.9559	-	-	-	-	-
Wavelet-SVM [58]	0.9391	-	-	0.9623	-	-

VI. CONCLUSION

This paper aims to identify and accurately locate single-phase to ground short circuit faults in power networks. To this end, the deep learning applications to interpret the TFs related to single-phase to ground short circuit faults are proposed. For this purpose, a standard IEEE transmission line has been used. The transmission line is divided into 6 equal segments so that each part represents one location (class). In all three phases of these segments, single-phase to ground short circuit faults were monitored and saved with different test impedances and voltage and current signals for each fault. The TF method was introduced and used to assess the effects of the fault impedances and fault location on the transmission line. In order to improve the TF method and extract the features in the TF traces, deep learning applications called CNN and the hybrid model of DRL were utilized to classify the faults. The TF traces were collected and used as input datasets for each network. After training and testing, the results of detecting and locating single-phase to ground short circuit faults indicated the superiority and efficiency of the hybrid model of DRL compared to CNN. DRL method passed the training and test stages with a correlation coefficient of R=98.51% and R=98.04%, respectively, while these results were observed in the conventional CNN, R=98.16% for training and R=96.12% for test. Then, in order to achieve the goal of early detection of single-phase to ground short circuit fault (high impedance), faults with high impedances (7000 and 9000 ohms) are implemented according to the previous routine in the transmission line. TF traces of new faults were used as inputs for test the saved networks. At this stage, the DRL method was R=96.61% more effective and powerful than the CNN method, which provided R=95.21% correlation coefficient. It should be noted that the use of learning methods can be an important step towards improving condition monitoring issues in power systems. Note that the presented method is non-pilot method and utilizes local data.

REFERENCES

[1] P. Gopakumar, M. J. B. Reddy, and D. K. Mohanta, "Adaptive fault identification and classification methodology for smart power grids using synchronous phasor angle measurements," *IET Gener., Transmiss. Distrib.*, vol. 9, no. 2, pp. 133–145, Jan. 2015.

[2] R. Godse and S. Bhat, "Mathematical morphology-based feature-extraction technique for detection and classification of faults on power transmission line," *IEEE Access*, vol. 8, pp. 38459–38471, 2020.

[3] M. Shahidehpour, F. Tinney, and Y. Fu, "Impact of security on power systems operation," *Proc. IEEE*, vol. 93, no. 11, pp. 2013–2025, Nov. 2005.

[4] S. Wang and P. Dehghanian, "On the use of artificial intelligence for high impedance fault detection and electrical safety," *IEEE Trans. Ind. Appl.*, vol. 56, no. 6, pp. 7208–7216, Nov. 2020.

[5] B. K. Chaitanya, A. Yadav, and M. Pazoki, "An intelligent detection of high-impedance faults for distribution lines integrated with distributed generators," *IEEE Syst. J.*, vol. 14, no. 1, pp. 870–879, Mar. 2020.

[6] J. An, C. Zhuang, F. Rachidi, and R. Zeng, "An effective EMTR-based high-impedance fault location method for transmission lines," *IEEE Trans. Electromagn. Compat.*, early access, May 25, 2020, doi: 10.1109/TEMC.2020.2991862.

[7] Q. Yang and I. Morrison, "Microprocessor-based algorithm for high-resistance earth-fault distance a protection," in *Proc. IEE Gener., Transmiss. Distrib.*, Nov. 1983, pp. 306–310.

[8] A. F. Elneweihi, E. O. Schweitzer, and M. W. Feltis, "Negative-sequence overcurrent element application and coordination in distribution protection," *IEEE Trans. Power Del.*, vol. 8, no. 3, pp. 915–924, Jul. 1993.

[9] X. Lin, J. Huang, and S. Ke, "Faulty feeder detection and fault self-extinguishing by adaptive petersen coil control," *IEEE Trans. Power Del.*, vol. 26, no. 2, pp. 1290–1291, Apr. 2011.

[10] Z. He, H. Zhang, J. Zhao, and Q. Qian, "Classification of power quality disturbances using quantum neural network and DS evidence fusion," *Eur. Trans. Electr. Power*, vol. 22, no. 4, pp. 533–547, May 2012.

[11] H. Teimourzadeh, B. Mohammadi Ivatloo, and M. Shahidehpour, "Adaptive protection of partially coupled transmission lines," *IEEE Trans. Power Del.*, early access, Mar. 30, 2020, doi: 10.1109/TPWRD.2020.2983138.

[12] T. Cui, X. Dong, Z. Bo, and A. Juszczyk, "Hilbert-transform-based transient/intermittent Earth fault detection in noneffectively grounded distribution systems," *IEEE Trans. Power Del.*, vol. 26, no. 1, pp. 143–151, Jan. 2011.

[13] X. Zeng, K. K. Li, W. L. Chan, S. Su, and Y. Wang, "Ground-fault feeder detection with fault-current and fault-resistance measurement in mine power systems," *IEEE Trans. Ind. Appl.*, vol. 44, no. 2, pp. 424–429, 2008.

[14] F. Gao and J. Cai, "Analysis for distributed generation impacts on current protection in distribution networks," *J. Electr. Power Sci. Technol.*, vol. 23, pp. 94–96, Sep. 2008.

[15] Y. Zhong, X. Kang, Z. Jiao, Z. Wang, and J. Suonan, "A novel distance protection algorithm for the phase-ground fault," *IEEE Trans. Power Del.*, vol. 29, no. 4, pp. 1718–1725, Aug. 2014.

[16] B. R. Bhalja and R. P. Maheshwari, "High-resistance faults on two terminal parallel transmission line: Analysis, simulation studies, and an adaptive distance relaying scheme," *IEEE Trans. Power Del.*, vol. 22, no. 2, pp. 801–812, Apr. 2007.
[17] H. Seyedi, P. Soleiman Nezhad, and S. Teimourzadeh, "Adaptive zero sequence compensation algorithm for double-circuit transmission line protection," *IET Gener., Transmiss. Distrib.*, vol. 8, no. 6, pp. 1107–1116, Jun. 2014.
[18] M. N. Alam, "Adaptive protection coordination scheme using numerical directional overcurrent relays," *IEEE Trans. Ind. Informat.*, vol. 15, no. 1, pp. 64–73, Jan. 2019.
[19] V. H. Makwana and B. R. Bhalja, "Digital distance relaying scheme for compensation of high resistance faults on double infeed transmission lines," in *Transmission Line Protection Using Digital Technology*. Cham, Switzerland: Springer, 2016, pp. 41–63.
[20] Y. Liang, Z. Lu, W. Li, W. Zha, and Y. Huo, "A novel fault impedance calculation method for distance protection against fault resistance," *IEEE Trans. Power Del.*, vol. 35, no. 1, pp. 396–407, Feb. 2020.
[21] X. Ma, X. Lin, F. Wei, Z. Li, Z. Wang, and Y. Ye, "A novel EHV transmission line protection of adequate fault-resistance sensitivity and faulted-phase selectivity," *Int. J. Electr. Power Energy Syst.*, vol. 118, Jun. 2020, Art. no. 105808.
[22] V. C. Nikolaidis, A. M. Tsimtsios, and A. S. Safigianni, "Investigating particularities of infeed and fault resistance effect on distance relays protecting radial distribution feeders with DG," *IEEE Access*, vol. 6, pp. 11301–11312, 2018.
[23] M. M. Eissa, "Ground distance relay compensation based on fault resistance calculation," *IEEE Trans. Power Del.*, vol. 21, no. 4, pp. 1830–1835, Oct. 2006.
[24] Z. Y. Xu, G. Xu, L. Ran, S. Yu, and Q. X. Yang, "A new fault-impedance algorithm for distance relaying on a transmission line," *IEEE Trans. Power Del.*, vol. 25, no. 3, pp. 1384–1392, Jul. 2010.
[25] S. Miao, P. Liu, and X. Lin, "An adaptive operating characteristic to improve the operation stability of percentage differential protection," *IEEE Trans. Power Del.*, vol. 25, no. 3, pp. 1410–1417, Jul. 2010.
[26] G. Luo, Y. Tan, M. Li, M. Cheng, Y. Liu, and J. He, "Stacked auto-encoder-based fault location in distribution network," *IEEE Access*, vol. 8, pp. 28043–28053, 2020.
[27] Y. Wang, Q. Li, and B. Chen, "Image classification towards transmission line fault detection via learning deep quality-aware fine-grained categorization," *J. Vis. Commun. Image Represent.*, vol. 64, Oct. 2019, Art. no. 102647.
[28] V. H. Ferreira, R. Zanghi, M. Z. Fortes, S. Gomes, and A. P. Alves da Silva, "Probabilistic transmission line fault diagnosis using autonomous neural models," *Electr. Power Syst. Res.*, vol. 185, Aug. 2020, Art. no. 106360.
[29] J. C. Arouche Freire, A. R. Garcez Castro, M. S. Homci, B. S. Meiguins, and J. M. De Morais, "Transmission line fault classification using hidden Markov models," *IEEE Access*, vol. 7, pp. 113499–113510, 2019.
[30] S. Zhang, Y. Wang, M. Liu, and Z. Bao, "Data-based line trip fault prediction in power systems using LSTM networks and SVM," *IEEE Access*, vol. 6, pp. 7675–7686, 2018.
[31] B. Li, J. Wu, L. Hao, M. Shao, R. Zhang, and W. Zhao, "Anti-jitter and refined power system transient stability assessment based on long-short term memory network," *IEEE Access*, vol. 8, pp. 35231–35244, 2020.
[32] K. Huang, Y. Wu, C. Wang, Y. Xie, C. Yang, and W. Gui, "A projective and discriminative dictionary learning for high-dimensional process monitoring with industrial applications," *IEEE Trans. Ind. Informat.*, vol. 17, no. 1, pp. 558–568, Jan. 2021.
[33] K. Huang, Y. Wu, C. Yang, G. Peng, and W. Shen, "Structure dictionary learning-based multimode process monitoring and its application to aluminum electrolysis process," *IEEE Trans. Autom. Sci. Eng.*, vol. 17, no. 4, pp. 1989–2003, Oct. 2020.
[34] E. Rahimpour, J. Christian, K. Feser, and H. Mohseni, "Transfer function method to diagnose axial displacement and radial deformation of transformer windings," *IEEE Trans. Power Del.*, vol. 18, no. 2, pp. 493–505, Apr. 2003.
[35] A. Moradzadeh and K. Pourhossein, "Application of support vector machines to locate minor short circuits in transformer windings," in *Proc. 54th Int. Universities Power Eng. Conf. (UPEC)*, Sep. 2019, pp. 1–6.
[36] A. Saito, M. Kuroishi, and H. Nakai, "Vibration prediction method of electric machines by using experimental transfer function and magneto-static finite element analysis," *J. Phys., Conf. Ser.*, vol. 744, Sep. 2016, Art. no. 012088.
[37] K. Jia, T. Bi, B. Liu, E. Christopher, D. W. P. Thomas, and M. Sumner, "Marine power distribution system fault location using a portable injection unit," *IEEE Trans. Power Del.*, vol. 30, no. 2, pp. 818–826, Apr. 2015.
[38] P. O'Shea, "The use of sliding spectral windows for parameter estimation in power system disturbance monitoring," *IEEE Trans. Power Syst.*, vol. 15, no. 4, pp. 1261–1267, 2000.
[39] A. Moradzadeh, K. Pourhossein, B. Mohammadi-Ivatloo, and F. Mohammadi, "Locating inter-turn faults in transformer windings using isometric feature mapping of frequency response traces," *IEEE Trans. Ind. Informat.*, early access, Aug. 17, 2020, doi: 10.1109/TII.2020.3016966.
[40] C. Lin, W. Gao, and M.-F. Guo, "Discrete wavelet transform-based triggering method for single-phase Earth fault in power distribution systems," *IEEE Trans. Power Del.*, vol. 34, no. 5, pp. 2058–2068, Oct. 2019.
[41] A. Moradzadeh and K. Pourhossein, "Location of disk space variations in transformer winding using convolutional neural networks," in *Proc. 54th Int. Univ. Power Eng. Conf. (UPEC)*, Sep. 2019, pp. 1–5.
[42] P. Li, Z. Chen, L. T. Yang, Q. Zhang, and M. J. Deen, "Deep convolutional computation model for feature learning on big data in Internet of Things," *IEEE Trans. Ind. Informat.*, vol. 14, no. 2, pp. 790–798, Feb. 2018.
[43] A. Moradzadeh and K. Pourhossein, "Short circuit location in transformer winding using deep learning of its frequency responses," in *Proc. Int. Aegean Conf. Electr. Mach. Power Electron. (ACEMP) Int. Conf. Optim. Electr. Electron. Equip. (OPTIM)*, Aug. 2019, pp. 268–273.
[44] Z. Zheng, Y. Yang, X. Niu, H.-N. Dai, and Y. Zhou, "Wide and deep convolutional neural networks for electricity-theft detection to secure smart grids," *IEEE Trans. Ind. Informat.*, vol. 14, no. 4, pp. 1606–1615, Apr. 2018.
[45] R. Liu, G. Meng, B. Yang, C. Sun, and X. Chen, "Dislocated time series convolutional neural architecture: An intelligent fault diagnosis approach for electric machine," *IEEE Trans. Ind. Informat.*, vol. 13, no. 3, pp. 1310–1320, Jun. 2017.
[46] K. Yang, X. Kong, Y. Wang, J. Zhang, and G. De Melo, "Reinforcement learning over knowledge graphs for explainable dialogue intent mining," *IEEE Access*, vol. 8, pp. 85348–85358, 2020.
[47] Y. He, Z. Zhang, F. R. Yu, N. Zhao, H. Yin, V. C. M. Leung, and Y. Zhang, "Deep-reinforcement-learning-based optimization for cache-enabled opportunistic interference alignment wireless networks," *IEEE Trans. Veh. Technol.*, vol. 66, no. 11, pp. 10433–10445, Nov. 2017.
[48] Y. He, N. Zhao, and H. Yin, "Integrated networking, caching, and computing for connected vehicles: A deep reinforcement learning approach," *IEEE Trans. Veh. Technol.*, vol. 67, no. 1, pp. 44–55, Jan. 2018.
[49] M. Glavic, "(Deep) reinforcement learning for electric power system control and related problems: A short review and perspectives," *Annu. Rev. Control*, vol. 48, pp. 22–35, 2019.
[50] V. Mnih, K. Kavukcuoglu, D. Silver, A. A. Rusu, J. Veness, M. G. Bellemare, A. Graves, M. Riedmiller, A. K. Fidjeland, G. Ostrovski, S. Petersen, C. Beattie, A. Sadik, I. Antonoglou, H. King, D. Kumaran, D. Wierstra, S. Legg, and D. Hassabis, "Human-level control through deep reinforcement learning," *Nature*, vol. 518, pp. 529–533, 2015.
[51] J. Woo and N. Kim, "Collision avoidance for an unmanned surface vehicle using deep reinforcement learning," *Ocean Eng.*, vol. 199, Mar. 2020, Art. no. 107001.
[52] E. Lin, Q. Chen, and X. Qi, "Deep reinforcement learning for imbalanced classification," *Appl. Intell.*, vol. 50, pp. 2488–2502, 2020.
[53] C. Feng, M. Sun, and J. Zhang, "Reinforced deterministic and probabilistic load forecasting via *Q*-learning dynamic model selection," *IEEE Trans. Smart Grid*, vol. 11, no. 2, pp. 1377–1386, Mar. 2020.
[54] R. E. Wilson and J. M. Nordstrom, "EMTP transient modeling of a distance relay and a comparison with EMTP laboratory testing," *IEEE Trans. Power Del.*, vol. 8, no. 3, pp. 984–992, Jul. 1993.
[55] A. E. Emanuel, D. Cyganski, J. A. Orr, S. Shiller, and E. M. Gulachenski, "High impedance fault arcing on sandy soil in 15 kV distribution feeders: Contributions to the evaluation of the low frequency spectrum," *IEEE Trans. Power Del.*, vol. 5, no. 2, pp. 676–686, Apr. 1990.
[56] A. Moradzadeh, A. Mansour-Saatloo, B. Mohammadi-Ivatloo, and A. Anvari-Moghaddam, "Performance evaluation of two machine learning techniques in heating and cooling loads forecasting of residential buildings," *Appl. Sci.*, vol. 10, no. 11, p. 3829, May 2020.
[57] X. Yuan, Y. Gu, Y. Wang, C. Yang, and W. Gui, "A deep supervised learning framework for data-driven soft sensor modeling of industrial processes," *IEEE Trans. Neural Netw. Learn. Syst.*, vol. 31, no. 11, pp. 4737–4746, Nov. 2020.
[58] U. B. Parikh, B. Das, and R. P. Prakash Maheshwari, "Combined wavelet-SVM technique for fault zone detection in a series compensated transmission line," *IEEE Trans. Power Del.*, vol. 23, no. 4, pp. 1789–1794, Oct. 2008.

HAMID TEIMOURZADEH (Student Member, IEEE) received the B.Sc. and M.Sc. degrees in electrical engineering from the University of Tabriz, Tabriz, Iran, in 2017 and 2020, respectively. His research interests include power system protection, planning, and economics.

ARASH MORADZADEH (Student Member, IEEE) was born in Tabriz, Iran, in 1991. He received the B.S. degree in electrical power engineering and the M.S. degree in power electronics and electrical machines from the Islamic Azad University of Tabriz, Tabriz, in 2016 and 2019, respectively. He is currently pursuing the Ph.D. degree in power electrical engineering with the University of Tabriz, Tabriz.

His current research interests include power and energy systems, cyber-physical systems, energy management, intelligent energy systems, transient in power systems, diagnostics and condition monitoring of power transformers, frequency response analysis, and application of data mining methods to design, and optimize and analysis of energy systems.

MARYAM SHOARAN studied medicine from 1990 to 1992, however, by pursuing her interest in computer science. She changed her field of study in 2001, and received the B.Sc. degree in computer engineering from Shahid Beheshti University, Tehran, Iran, in 2005, and the M.Sc. and Ph.D. degrees in computer science from the University of Victoria (UVic), Canada, in 2007 and 2011, respectively. After two years of postdoctoral research at UVic, she came back to Iran. She currently works as an Assistant Professor with the Department of Mechatronics Engineering, University of Tabriz, Tabriz, Iran.

BEHNAM MOHAMMADI-IVATLOO (Senior Member, IEEE) received the B.Sc. degree (Hons.) in electrical engineering from the University of Tabriz, Tabriz, Iran, in 2006, and the M.Sc. and Ph.D. degrees (Hons.) from the Sharif University of Technology, Tehran, Iran, in 2008. He is currently a Professor with the Faculty of Electrical and Computer Engineering, University of Tabriz. His main areas of research include the economics, operation, and planning of intelligent energy systems in a competitive market environment.

REZA RAZZAGHI (Member, IEEE) received the Ph.D. degree in electrical engineering from the Swiss Federal Institute of Technology of Lausanne (EPFL), Lausanne, Switzerland, in 2016. In 2017, he joined Monash University, Melbourne, Australia, where he is currently a Lecturer (Assistant Professor) with the Department of Electrical and Computer Systems Engineering. His research interests include power system protection and control, microgrids, and electromagnetic transients in power systems. He was a recipient of the 2013 Basil Papadias Best Paper Award from the IEEE PowerTech Conference and the 2019 Best Paper Award of the IEEE TRANSACTIONS ON ELECTROMAGNETIC COMPATIBILITY.